



14<sup>TH</sup> CANADIAN MASONRY SYMPOSIUM  
MONTREAL, CANADA  
MAY 16<sup>TH</sup> – MAY 20<sup>TH</sup>, 2021



## IN-PLANE SEISMIC BEHAVIOR OF SPECIAL REINFORCED FULLY GROUTED MASONRY SHEAR WALLS SUBJECTED TO HIGH AXIAL LOADS

Mahmood, Tousif<sup>1</sup>; Gheni, Ahmed A.<sup>2</sup> and ElGawady, Mohamed<sup>3</sup>

### ABSTRACT

The flexural behavior of full scale fully grouted special reinforced masonry shear walls, which are exceeding the axial load limits and maximum reinforcement criteria of TMS 402/602 has been investigated. This is part of an ongoing research that focuses to overcome the issues in the design of intermediate and special reinforced masonry shear walls according to current TMS 402 provisions, which limits the flexural reinforcement ratio. The walls have been subjected to relatively heavy axial loading that equal to 1.5 times the allowed axial load limit per the TMS code. This posed a very practical design issue where the  $\rho_{\max}$  as per TMS 402/602 becomes less than  $\rho_{\text{provided}}$  or even negative. The examined walls met the design requirements for special reinforced masonry shear walls. The walls were tested to failure under in-plane cyclic lateral loading to investigate the effects of the level of axial compressive stress on the inelastic behavior and ductility of the three walls out of which two were non-conforming to TMS 402/602. Tensile yielding of the vertical reinforcement has been observed for walls non confirming to TMS 402/602 along with the characteristic formation of plastic hinge zone at the bottom of the walls. Experimental findings of these full-scale walls have found TMS 402 to be conservative on design parameters such as masonry strain at failure, tensile strain factor and axial load limits.

**KEYWORDS:** *Reinforced Masonry, Shear walls, Fully Grouted, Ductility, Seismic Loads, TMS*

---

<sup>1</sup>Ph.D Candidate, Civil, Architectural and Environmental Engineering Department, Missouri University of Science and Technology, Rolla, MO 65401, U.S.A., tmrkw@mst.edu

<sup>2</sup>Lecturer, Civil Engineering Department, Komar University of Science and Technology, Sulaymaniyah, Iraq., ahmed.gheni@komar.edu.iq

<sup>3</sup> Professor and Benavides Faculty Scholar, Civil, Architectural and Environmental Engineering Department, Missouri University of Science and Technology, Rolla, MO 65401, U.S.A., elgawadym@mst.edu

## INTRODUCTION

With increased safety requirements of building codes for structures under severe seismic action, a lot of research is currently undertaken to evaluate the behavior and performance of critical seismic force-resisting elements such as shear walls. The prevailing seismic design philosophy for reinforced masonry shear walls (RMSWs) assumes that adequate seismic performance is achieved with increased ductility allowing more energy dissipation. This is true for structural elements failing in flexural as it has shown more ductile behavior with characterized tensile yielding of vertical reinforcement along with formation of plastic hinges and toe crushing of RMSWs[1-3]. However, with increased flexural reinforcement, the masonry may reach critical compression strain before yielding of the reinforcement and eventually leading to brittle failure[4]. Brittle shear failure and significantly decreased ductility have also been predominant with increased axial load[2, 3]. As a result, current code provisions limit the amount of flexural reinforcement and axial load to ensure proper ductility in masonry walls controlled by flexural behavior.

While the TMS 402/602 [5] provisions ensure ductile behavior, it poses significant issue for design engineers when masonry walls are heavily axially loaded. In many practical situations, the current TMS 402/602 approach resulted in a maximum reinforcement ratio that is less than the required minimum reinforcement ratio. This is particularly true for intermediately and specially reinforced shear walls which are RMSWs having special details to be used in moderate to high seismic regions. Therefore, it is not possible to use strength design of the TMS 402/602 to design such elements when subjected to heavy axial loads. Moreover, these limits were developed based on experience with fully grouted masonry walls.

There is no single comprehensive experimental study investigating the current TMS 402/602 maximum reinforcement ratio,  $\rho_{\max}$ , provisions and the performance of RMSWs having flexural tensile reinforcement ratios exceeding  $\rho_{\max}$ . The research reported in this investigation is an evaluation of the performance of fully grouted masonry walls having axial compressive stress ratio violating the  $\rho_{\max}$  provision in TMS 402/602.

## RESEARCH SIGNIFICANCE

The current strength design provisions of TMS 402 proposes equation 1 for  $\rho_{\max}$  for fully grouted walls with concentrated tension reinforcement. However, with increased axial load this equation have yielded values of  $\rho_{\max}$  less than  $\rho_{\text{provided}}$  and even negative in certain cases.

$$\rho_{\max} = \frac{0.64 I_m \left( \frac{\epsilon_{mu}}{\epsilon_{mu} + \alpha \epsilon_y} \right) \frac{P}{bd}}{f_y} \quad (1)$$

This means with current code provisions masonry cannot be used for high rise construction, which in turn is sacrificing the compression capacity of masonry. With very limited work on large scale reinforced masonry shear walls subjected to heavy axial loads, this research aims to study the behavior of such walls and make necessary amendments to the aforementioned  $\rho_{\max}$  provisions.

## EXPERIMENTAL PROGRAM

The results of three full-scale fully grouted reinforced masonry shear walls subjected to in-plane cyclic loading are presented in this paper. All the three walls had same vertical and horizontal reinforcement ratio to study the effect of axial compressive stress. These three walls are categorized as special reinforced shear walls as per TMS 402/602.

### *Wall specimen description*

Standard 203 mm (8 inch) CMU blocks were used to construct the walls that were 1829 mm (72 inches) in length and 3048 mm (120 inches) high. All the walls tested had an aspect ratio of 1.5 to achieve flexure dominated behavior with the lateral cyclic load being applied at 2743 mm (108 inches) from bottom of the wall (Figure 1b). Each wall consisted of 4.5 blocks long and 13.5 courses high. The vertical reinforcement of the wall extended from the foundation all the way through the height of the wall. For facilitating the un-spliced vertical reinforcement, open end CMUs (A blocks) were used as shown in Figure 1a and extended to full wall height from wall foundation to eliminate any effect of splicing on test results. Horizontal shear reinforcement ( $\rho_h=0.11\%$ ) was provided in bond beams. Knockout blocks bond beams were placed at a spacing of 610 mm (24 inches) for each wall. The shear rebar was anchored with TMS 402/602 provisions-compliant 180-degree hooks around the outermost vertical reinforcement. Both the vertical and horizontal reinforcement ratio as per equation 2 and 3 have been kept constant for all three walls. The specimen ID for the walls – FG-IP-XX-YY consist of two parts. The notation ‘XX’ refers to spacing of vertical reinforcement and ‘YY’ refers to the axial compressive stress percentage on the walls. The summary for wall details are given in Table 1.

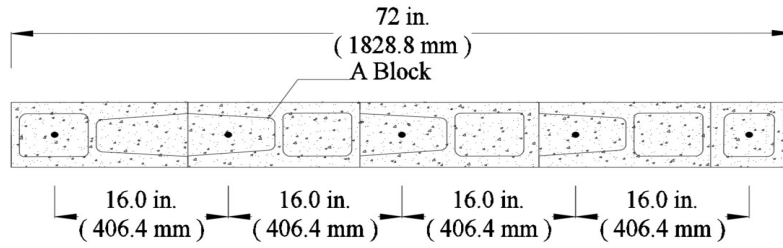
$$\rho_v = \frac{A_s}{A_g} \quad (2)$$

$$\rho_h = \frac{A_{sh}}{st} \quad (3)$$

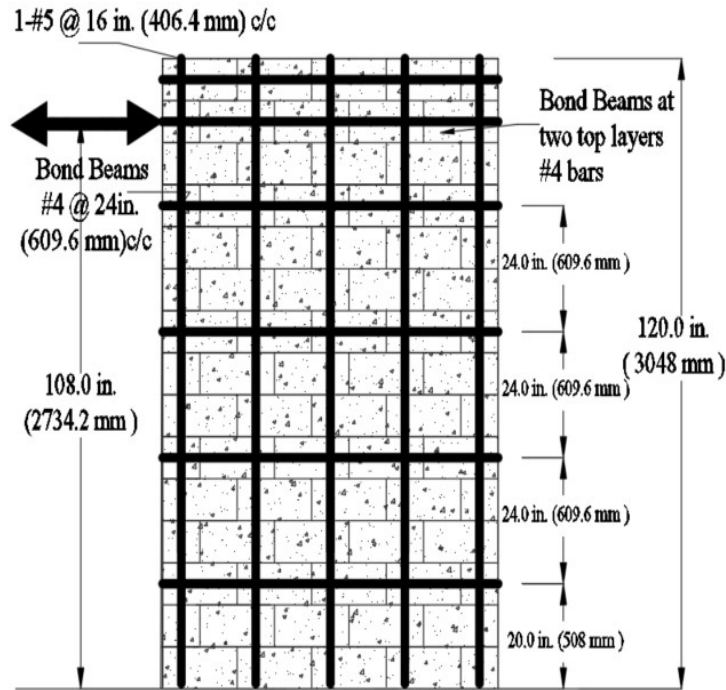
Where  $A_s$  is the total provided vertical reinforcement,  $A_g$  is the gross cross sectional area,  $A_{sh}$  is the provided horizontal reinforcement, ‘s’ is the distance between bond beams and ‘t’ is the wall thickness.

### *Material Characterization*

Walls were built in running bond and face shell bedding. Two-block high grouted prisms were constructed in stack bond as per TMS 402/602 to determine the wall properties. The material properties of prisms, grout samples, mortar and the steel reinforcement are presented in Table 2 as per respective ASTM standards.



(a)



(b)

**Figure 1: (a) Wall cross-section details, (b) Wall geometry details**

The walls were subjected to fully reversed in-plane cyclic load using two 890kN (200-kips) actuators as shown in Figure 2a. Loading protocol as per FEMA 461[6] have been used. The amplitude  $a_i$  of the stepwise increasing deformation cycles is given by the equation  $a_{i+1} = 1.4a_i$ , where  $a_i$  is the amplitude at 'i' cycle as shown in Figure 2b. The axial stress on the walls were applied with a steel loading beam equipped with load cells and high strength post tensioning strands that run through the RC pedestal. The post tensioning force on the strands were monitored thorough the load cells.

**Table 1: Wall summary details**

Wall	Vertical reinforcement			Axial compressive stress percentage	Remark based on TMS 402/602 code provisions for axial load limit	Remark based on TMS 402/602 code provisions of $\rho_{max}$
	Number and size	$\rho_v$ (%)	$\rho_{max}$ as per TMS 402/602 (%)	( $\% \frac{P}{f_m A_n}$ )		
FG-IP-16-03	#5 x 5 cells (5 x 200 mm <sup>2</sup> )	0.28	0.31	03	Allowed	OK
FG-IP-16-10	#5 x 5 cells (5 x 200 mm <sup>2</sup> )	0.28	0.11	10	Allowed	$\rho_{v,provided} > \rho_{max}$
FG-IP-16-15	#5 x 5 cells (5 x 200 mm <sup>2</sup> )	0.28	-0.04	15	Not allowed	$\rho_{v,provided} > \rho_{max}$

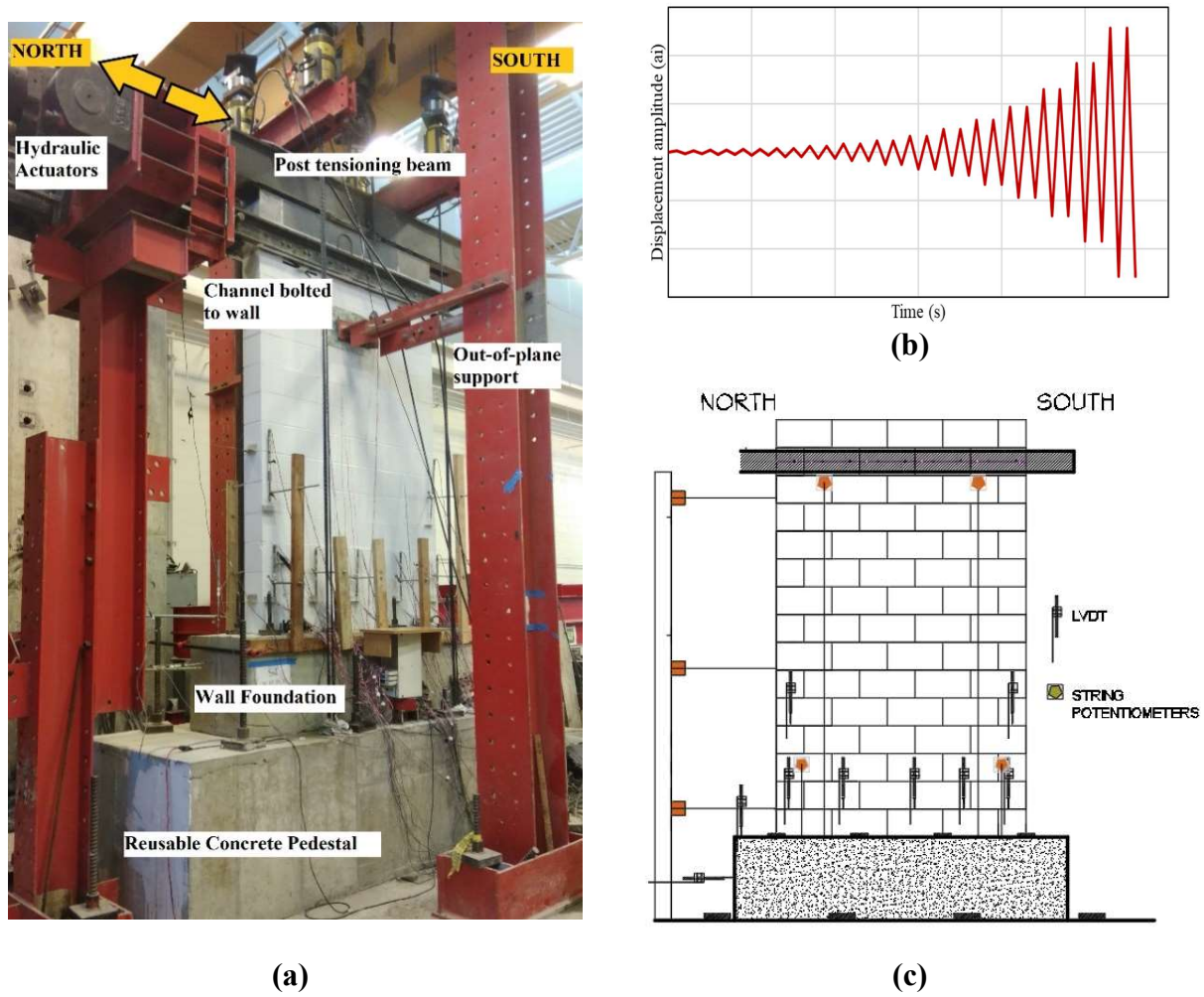
**Table 2: Material Properties**

Items	Standard Tests	Results	
Mortar (type S)	ASTM C39 / C39M-18	$f'_c = 14$ MPa (2030 psi)	
Grout	ASTM C1019-18	$f'_g = 26.5$ MPa (3850 psi)	
Masonry block prism (fully grouted)	ASTM C1314-18	Stretcher block prisms	$f'_m = 16.5$ MPa ( 2400 psi)
		A block (open end) prisms	$f'_m = 15$ MPa (2200 psi)
		End block (half unit) prisms	$f'_m = 15$ MPa ( 2200 psi)
Steel Reinforcement	A615/A615M – 18	$f_y = 462$ MPa ( 67000 psi)	

***Test Setup, Loading and Instrumentation***

Figure 2a shows the test setup of the walls being tested. The wall foundation was post tensioned to a larger reinforced concrete pedestal with 8 Dywidag bars which in turn was post tensioned to the laboratory's strong floor. The out-of-plane bracing used is shown in Figure 2a. The out-of-plane supports had Teflon sheet in contact with wall surface to eliminate any frictional resistance between the support and the wall.

A computerized data acquisition system was used to measure the applied loads, horizontal and vertical displacements measured using several string potentiometers and LVDTs. A total of eleven LVDTs and four string potentiometers (Figure 2c) were installed along the wall length and height to monitor the vertical displacements with respect to the wall foundation. Moreover, two more LVDTs were used to separately measure the sliding and rocking of the foundation. Eleven strain gauges were attached to each vertical reinforcement bar. The strain gauges were placed in close proximity at the plastic hinge length region to accurately measure the strain profile in the plastic hinge region. Out of the eleven strain gauges, three were attached on the reinforcement inside the foundation to determine the strain penetration inside the foundation.



(a) (b) (c)  
**Figure 2: (a) Test Setup, (b) Loading protocol, (c) Instrumentation**

## TEST RESULTS AND DISCUSSION

### *Hysteretic behavior and failure events*

The FG-IP-16-03 wall was subjected to 3% axial stress conforming to TMS 402/602. Figure 3a shows the load-displacement hysteresis. The specimen showed a complete flexural failure with vertical splitting cracks at the onset of yielding and toe crushing under compression at 2-3 times

of yielding strain. Widening of bed joint cracks along with vertical splitting cracks at the south bottom end were observed at a drift of 0.70% which is at the onset of yielding. With drift reaching 1%, more step cracks appeared and widening of the 2nd course bed joint. At 1.75% drift level compression cracks widened with bar buckling evident as masonry up to 3rd course was bulging out with severe splitting cracks (Figure 4a and 4b) on both ends of the wall. The wall continued at this peak load of 253.5 kN (57 kips) for 2 more cycles reaching a drift of 2.6%. The load degradation observed was not rapid. The wall sustained almost 70% of the peak load in the last two cycles reaching a maximum drift of 3.50%. Maximum crack width of 18mm (0.70 inch) was recorded at this drift level. The maximum masonry strain recorded at the wall toe at failure was 0.0067. The outermost vertical rebars has gone through almost 7 times of the yielding strain and buckling of rebar revealed with masonry spalling (Figure 4b). The extent of damage at the end of the test is shown in Figure 4c.

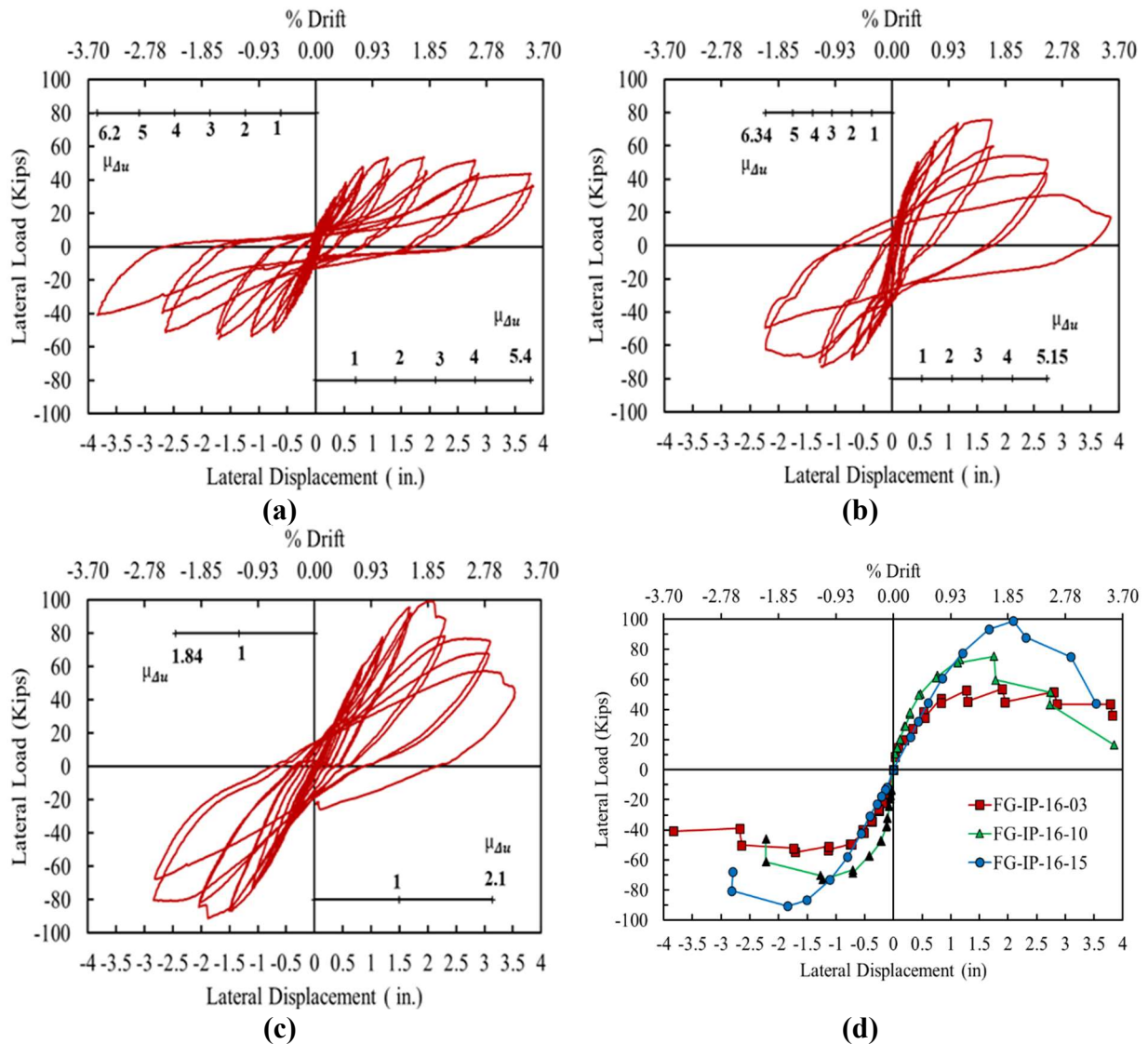


**Figure 3: Load displacement hysteretic response (a) FG-IP-16-03, (b) FG-IP-16-10, (c) FG-IP-16-15, (d) Load-displacement envelopes for the walls**

FG-IP-16-10 wall was subjected to 10% axial stress (highest axial load limit as per TMS 402) and is non-confirming to TMS 402/602 with  $\rho_{max}$  less than  $\rho_{provided}$ . Figure 3b shows the load-displacement hysteresis. Followed by step cracks extending up to 6th course at a drift of 0.52%. Compression cracks were observed at the south bottom corner at a drift level of 0.70% which is evidently at the onset of yielding. The south bottom corner experienced masonry crushing as the wall neared peak load at 1.17% drift as shown in Figure 4d. At this stage bar buckling was observed as the wall reached peak 335 kN (75.4 kips) at 1.62% drift. Diagonal tensile cracks (Figure 4e) were seen along with the bulging of cracked masonry at the north end was also observed reaching a drift of 2% in this direction. Diagonal shear cracks and step cracks extended up to the 6th course which is the bond beam and vertically reaching to the anchorage of the hooks at the 12th course bond beam. The shear strain recorded in these two courses were 0.4 and 0.8 times the yield strain respectively. At drift of 1.45% in north direction, out-of-plane deformation of the bottom three courses were noticed accompanied with slight drop in lateral load. At the next cycle severe masonry crushing was observed at the north corner at load degradation of 30% reaching a drift of 2.5%. The maximum masonry strain recorded at the wall toe was 0.0065. The outermost vertical rebars showed up to 5 times of yielding strain at both ends. The extent of damage at the end of the test is shown in Figure 4f.

FG-IP-16-15 wall was subjected to heavy axial stress of 15% (exceeding TMS 402 axial load limit by 1.5 times) and is non-confirming to TMS 402/602 with  $\rho_{max}$  less than  $\rho_{provided}$ . Figure 3c shows the load-displacement hysteresis. With increased drift, masonry toe compression at the south end was seen at drift of 1.65% as shown in Figure 4g. At the same half cycle, vertical compression cracks were observed at the north end as well. The wall reached its peak strength of 440 kN (99 kips) at a drift of 1.85%. Crushing of the masonry at both toe region evidently showed bar buckling up to the 2nd course as shown in Figure 9b. Bar yielding of up to 5 times of yield strain was recorded in both the outermost rebars reaching up to the 3rd course. Almost 30% load degradation is observed reaching a drift of 2.80%. At this stage more shear cracks appeared (Figure 4h) up to the 6th course bond beam and reaching up to the 12th course. The shear strain in the bond beam of the 6th course reached up to 1.1 times the yield strain at this peak load degradation phase. The maximum masonry strain recorded at the wall toe was 0.0056. The yielding recorded on each of the outermost rebars reached up to almost 5 times of yield strain. The extent of damage at the end of test is shown in Figure 4i.





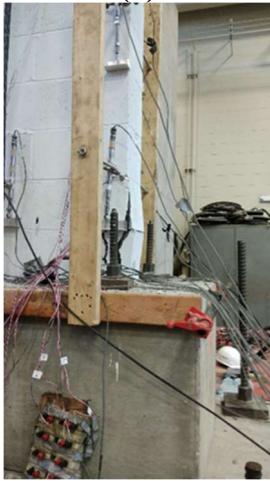
(a)



(b)



(c)



(d)



(e)



(f)



(g)



(h)



(i)

**Figure 4: Cracking and damage of wall specimen : (a) and (b) Crushing and bar buckling of FG-IP-16-03, (c) Extent of damage at end of test of FG-IP-16-03, (d) and (e) Crushing and masonry spalling of FG-IP-16-10, (f) Extent of damage at end of test of FG-IP-16-10, (g) and (h) Compression cracks and bar buckling of FG-IP-16-15, (i) Extent of damage at end of test of FG-IP-16-15.**

### ***Load-displacement response***

Figure 3d shows the load-displacement envelopes for the walls. The effects of axial compression stress can be seen here. The backbone curves of these specimens have been obtained using the procedure detailed in FEMA 356[7]. For these special reinforced walls, the initial stiffness and flexural yield strength increased with increasing axial compressive stress. This may be attributed to the fact that the opening of the flexural cracks is significantly reduced by application of axial load [8]. Moreover, higher drift percent was observed in walls that were subjected to 3% and 10 % axial stress. Fewer displacement cycles were sustained at the load degradation phase for the walls subjected 15% axial stress which is inconsistent with findings of Ahmadi et al.[9] on walls subjected to 15% axial load.

### ***Displacement ductility***

Displacement ductility, defined as the ultimate to effective yield deformations [1], is crucial for seismic design. However, there have been no consensus on the appropriate definition of yield and ultimate displacements. An equivalent elastic-perfectly plastic system is used in this paper to assume a bi-linear approximation of the load-displacement response as per the method proposed by FEMA 356 [7]. The displacement ductility values calculated at maximum load, and at 20% strength degradation, are presented in Table 3.

Wall ID	Loading direction	$\mu_{\Delta u}$	$\mu_{\Delta 0.8u}$
FG-IP-16-03	(+) ve	2.70	5.40
	(-) ve	2.76	6.18
FG-IP-16-10	(+) ve	3.30	5.15
	(-) ve	3.51	6.34
FG-IP-16-15	(+) ve	1.39	2.07
	(-) ve	1.38	2.11

Note: (+)ve loading direction - Push towards south  
(-)ve loading direction - Pull towards north

Displacement ductility values reduced with increasing the axial compressive stress. This can be attributed to delayed yielding of the tensile reinforcement as well as reaching compression failure at lower curvatures[8] for the walls subjected to 10% and 15% axial load. At the maximum load, the drop in the displacement ductility was almost 48% as axial compressive stress was increased from 3% to 15%. At 15% axial compressive stress,  $\mu_{\Delta 0.8u}$  was 2 and exceeding drift of 1.5% at 20% strength degradation. Bar buckling observed near the wall-foundation interface (fixed support conditions) for the higher axial loads contributed to reduction in flexural ductility at higher axial compressive stress.

## **CONCLUSIONS**

Three large scale fully grouted slender RMSWs subjected to axial loads of 3, 10 and 15% were tested under cyclic in-plane loading. Two of the heavily axially walls (10% and 15%) do not satisfy the  $\rho_{max}$  provision and the last wall (15% axially loaded) do not confirm to the axial load limit of

TMS 402. These experimental work on large scale specimen tries to fill in the gap in literature for conservative and unverified limits on axial load and maximum reinforcement provisions by TMS 402. Following conclusions are drawn from the tests:

- All three walls tested displayed flexural failure with yielding of vertical reinforcement exceeding yield strains significantly at the toe of the wall.
- The maximum strain in masonry recorded at failure for 10% and 15% axially loaded walls were 2-2.5 times the design ultimate masonry strain of  $\epsilon_{mu}=0.0025$  prescribed by TMS 402.
- The outermost vertical reinforcement underwent yielding at a factor of 7,5 and 5 times the yield strain compared to the TMS 402 design limit of 4 for special reinforced walls for the axial load ratio of 3%, 10% and 15% respectively.
- The heavily axially loaded walls (10% and 15) displayed flexural failure however, the 15% axially loaded wall showed rapid strength degradation after going through 3 times the yielding strain.
- The displacement ductility of 15% axially loaded wall dropped by almost 50% at peak load compared to the 10% axially loaded wall. The investigated walls displayed a displacement ductility values of 2.70, 3.30, and 1.39 for walls axially loaded at 3%, 10%, and 15% respectively.

## ACKNOWLEDGEMENTS

This research was conducted by Missouri University of Science and Technology and was supported by the National Concrete Masonry Association (NCMA). However, all opinions, findings, and conclusions expressed in this publication are those of the authors. They are not necessarily those of the NCMA.

## REFERENCES

- [1] Paulay, T. and M.J.N. Priestley, *Seismic Design of Reinforced Concrete and Masonry Buildings*, ISBN: 978-0-471-54915-4. 1992
- [2] Shedid, M.T., R.G. Drysdale, and W.W. El-Dakhakhni, *Behavior of Fully Grouted Reinforced Concrete Masonry Shear Walls Failing in Flexure: Experimental Results*. Journal of Structural Engineering, 2008. 134(11): p. 1754-1767.
- [3] Shing, P.B., et al., *Inelastic behavior of concrete masonry shear walls*. 1989. 115(9): p. 2204-2225.
- [4] Eikanas, I.K., *Behavior of concrete masonry shear walls with varying aspect ratio and flexural reinforcement*. 2003.
- [5] TMS(2016). *Building Code Requirements for Masonry Structures and Specification for Masonry Structures, TMS 402/602*. The Masonry Society, Longmont, CO, USA.
- [6] FEMA, *Interim Testing Protocols for Determining the Seismic Performance Characteristics of Structural and Nonstructural Components*, Report No. FEMA-461. 2007.
- [7] FEMA, *FEMA 356 - Prestandard and commentary for the seismic rehabilitation of buildings*, FEDERAL EMERGENCY MANAGEMENT AGENCY. Report FEMA-356, Washington, DC, 2000.

- [8] Shing, P., M. Schuller, and V.J.J.o.s.E. Hoskere, *In-plane resistance of reinforced masonry shear walls*. 1990. 116(3): p. 619-640.
- [9] Ahmadi, F., et al., *Seismic performance of cantilever-reinforced concrete masonry shear walls*. *Journal of Structural Engineering (United States)*, 2014. 140(9): p. 1-18.